Available online at www.sciencedirect.com
ScienceDirect
International Journal of Heat and Mass Transfer 50 (2007) 1603–1615
International Journal of HEAT and MASS TRANSFER
www.elsevier.com/locate/ijhmt

Taylor dispersion coefficients for laminar, longitudinal flow past arrays of circular tubes

Sangkyun Koo *

Research Park, LG Chem, Ltd., Science Town, Daejeon 305-380, Republic of Korea

Received 22 June 2005; received in revised form 3 April 2006
Available online 13 November 2006

Abstract

The problem of determining shell-side Taylor dispersion coefficients for a shell-and-tube configuration is examined in detail for both ordered as well as disordered arrangement of tubes. The latter is modeled by randomly placing N tubes within a unit cell of a periodic array. It is shown that shell-side Taylor dispersion coefficient D_T is expressed by $D_T = D_M(1 + \lambda Pe^2)$ and the coefficient λ is divergent with N, where D_M is the molecular diffusivity of solute on the shell side and Pe is the Peclet number given by aU/D_M with a and U being the radius of tube and the mean fluid velocity on the shell side, respectively. The coefficient λ depends on the spatial average and the fluid velocity weighted average of the concentration of solute on the shell side. The behavior of the coefficient λ with N arises due to logarithmically divergent nature of concentration disturbances caused by each tube in the plane normal to the axes of the tubes. An effective-medium theory is developed for determining conditionally-averaged velocity and concentration fields and hence the shell-side Taylor dispersion coefficients. Its predictions are compared with the results of rigorous numerical computations. The present study also presents formulas for determining the shell-side Taylor dispersion coefficients for square and hexagonal arrays of tubes with cell theory approximations.

Keywords: Taylor dispersion coefficient; Shell-and-tube configuration; Effective-medium theory; Conditional average; Cell theory; Multipole expansion method

1. Introduction

Shell and tube configurations are widely used in heat and mass transfer equipments such as hollow fiber modules used in gas separation by membranes and heat exchangers. Recently these configurations are utilized even as a chemical reactor in a microfluidic system [1]. In spite of their widespread use in practice, theoretical studies to predict the transport properties such as heat (or mass) transfer coefficients and Taylor dispersion coefficients for the process using the configurations are not many. Sangani and Acrivos [2] determined the heat transfer coefficient for the shell side for the case when the mean flow direction is perpendicular to the tubes in the limit of small Peclet and small Reynolds numbers and that in the limit of small Reynolds number but large Peclet number was obtained by Wang and Sangani [3]. For the longitudinal flow parallel to the axes of tubes Sparrow et al. [4] determined the shell-side heat transfer coefficients for the periodic arrays of tubes. The case of random arrays of tubes was examined by Koo and Sangani [5] to determine the mass transfer coefficients for the shell side. They obtained shell-side Sherwood numbers for longitudinal flow along the axes of tubes inside which a fluid flows countercurrently in a hollow-fiber contactor.

Another important mass transfer phenomenon encountered in chemical processes is Taylor dispersion. The present study deals with the problem of determining shell-side Taylor dispersion coefficients for laminar flow parallel to the axes of tubes. The tube walls are assumed to be

* Tel.: +82 42 866 5705; fax: +82 42 862 6069.
E-mail address: skkoo@lgchem.com

0017-9310/$ - see front matter © 2006 Elsevier Ltd. All rights reserved.
doi:10.1016/j.ijheatmasstransfer.2006.08.032

Nomenclature

A_s	area occupied by the shell side fluid
a	radius of tubes
c	concentration of solute on shell side
D_M	molecular diffusivity
D_T	Taylor dispersion coefficient
f	solute concentration on the shell side as a function of $\mathbf{x}_1$ and $\mathbf{x}_2$
$g(r)$	radial distribution function
G	pressure gradient non-dimensionalized by $\mu U/a^2$ in axial direction of tubes
$P(\mathbf{r}\|\mathbf{0})$	probability of finding a tube at the distance $\mathbf{r}$ from the origin given a tube at origin $\mathbf{0}$
Pe	Peclet number based on shell-side flow
r	radial distance from the center of the tube at origin
R	exclusion radius in effective-medium model
R_c	radius of fluid cell in cell model
R_s	radius of shell
$S(\mathbf{0})$	structure factor at zero wavenumber limit
U	superficial velocity of the fluid on the shell side
u	fluid velocity on the shell side
$\mathbf{x}^\alpha$	position vector of the center of tube α
$\mathbf{x}_L$	coordinates (position vector) of the lattice points of the array
$\langle u\rangle_s$	spatial average of u over shell side
$\langle a_n\rangle$	average of coefficients a_n over N tubes in a unit cell
$\langle A_n\rangle$	average of multipoles A_n over N tubes in a unit cell
$\langle u\rangle_0$	unconditionally averaged velocity, u
$\langle u\rangle_1$	conditionally averaged velocity, u

Greek symbols

χ	indicator function
δ	Dirac's delta function
ϕ	area fraction of the tubes
ρ	density of the shell fluid
τ	unit cell area non-dimensionalized by a^2
μ	viscosity of fluid
μ_B	Brinkman viscosity
ψ	product of velocity and concentration satisfying Eq. (35)

non-absorbing and non-reacting. Both the periodic and the random arrangement of tubes are considered. The case of random arrays is examined by generating hard-disk configurations of N non-overlapping disks placed within a unit cell of a periodic array and computing Taylor dispersion coefficient for each configuration. It is found that Taylor dispersion coefficient is logarithmically divergent with N. This logarithmic divergence arises from the fact that the fundamental singularity for Laplace equation in a two-dimensional space corresponding to a point source of mass is $\log r$, r being the distance from the source. For the fully developed case the concentration outside the tubes satisfies Poisson equation with the strength of the source or sink related to the fluid velocity and the area fraction of tubes in the unit cell. The conditionally-averaged concentration field obtained by averaging over all configurations of tubes with the position of one of the tubes fixed at, say, origin satisfies therefore Laplace equation at great distances from the tube. Detailed analysis of the source and sink near the tube, however, shows a non-zero net source leading to the aforementioned logarithmic divergence.

It is practically useful to confirm the occurrence of such logarithmic divergence experimentally. However it seems that the relevant experimental observation has not been reported yet. Instead, a set of experiments carried out by Yang and Cussler [6] may be considered as an indirect evidence confirming that the behavior of the logarithmic divergence can be observed in real situations although their experiments are concerned with a different problem which is to determine shell-side Sherwood number for the longitudinal laminar flow in a countercurrent hollow-fiber contactor. In their experiment, it is found that the shell-side Sherwood number is unexpectedly small, i.e., 0.08 when the number of tubes (fibers) is 2100 in a hollow fiber module. And this result was not clearly explained in their paper. Later Koo and Sangani [5] have shown that the shell-side Sherwood number becomes vanishingly small as the number of tubes increases due to the divergent nature of concentration disturbance caused by each tube in the plane normal to its axis. This behavior of shell-side Sherwood number results from the fact that the governing equation for the concentration field on the shell side is also given in the form of Laplace equation with source and sink in two dimensional space, which is similar to the case of the present study. The shell-side Sherwood number by Koo and Sangani's analysis is 0.09 for the experimental condition given by Yang and Cussler [6], which accounts for the experimental results well.

An exact expression is derived for the coefficient of logarithmic dependence that depends on the conditionally-averaged velocity outside a tube fixed at origin. An effective-medium theory is developed for predicting the conditionally-averaged velocity and concentration field and hence the coefficient of logarithmic dependence of Taylor dispersion coefficient. The theory is shown to be in good qualitative agreement with the simulation results. The simulation results for Taylor dispersion coefficients for square and hexagonal array are compared also with a cell theory approximation. Agreement between the theory and numerical results is excellent at small area fractions. At larger area fractions, the cell theory gives better estimates for hexagonal arrays.

2. Formulation of the problem and the method

The present study deals with the problem of determining the shell-side axial dispersion coefficient resulting from the combination of molecular diffusion of a solute in the plane normal to the tubes and the variations in the axial velocity of the fluid in a shell-and-tube configuration as shown in Fig. 1. The solute concentration c satisfies the usual convection–diffusion equation

$$\frac{\partial c}{\partial t} + u\frac{\partial c}{\partial x_3} = D_{\mathrm{M}}\nabla^2 c, \tag{1}$$

where D_{M} is the molecular diffusivity of the solute in the shell side fluid. We take x_3-axis to be along the axes of the tubes and (x_1, x_2) to be the coordinates of a point in the plane normal to the tubes. The distances are non-dimensionalized by a, the radius of the tubes. And the axial velocity of fluid on the shell side is denoted by u. The average concentration of the solute $\langle c\rangle_{\mathrm{s}}$ defined by

$$\langle c\rangle_{\mathrm{s}} = \frac{1}{(1-\phi)\tau}\int_{A_{\mathrm{s}}} c\,\mathrm{d}A \tag{2}$$

satisfying a similar equation

$$\frac{\partial\langle c\rangle_{\mathrm{s}}}{\partial t} + \langle u\rangle_{\mathrm{s}}\frac{\partial\langle c\rangle_{\mathrm{s}}}{\partial x_3} = D_{\mathrm{T}}\frac{\partial^2\langle c\rangle_{\mathrm{s}}}{\partial x_3^2} \tag{3}$$

with D_{T} being the Taylor dispersion coefficient. Here, τ is the area of the unit cell non-dimensionalized by a^2, ϕ is the area fraction of the tubes, and A_{s} is the area occupied by the shell side fluid. The spatial average over the shell side area is denoted by a subscript s outside the angular brackets. The average velocity of the fluid on the shell side is $\langle u\rangle_{\mathrm{s}} = U/(1-\phi)$, U being the superficial velocity. Since the above equations are linear we may choose a relatively simple form of $\langle c\rangle_{\mathrm{s}}$ to evaluate the Taylor dispersion coefficient. We follow Koch and Brady [7] and take

$$\langle c\rangle_{\mathrm{s}} = (x_3 - \langle u\rangle_{\mathrm{s}} t)/U, \tag{4}$$

which clearly satisfies Eq. (3). Now substituting

$$c = \langle c\rangle_{\mathrm{s}} + a^2 f(x_1, x_2)/D_{\mathrm{M}} \tag{5}$$

into Eq. (1) we obtain

$$\frac{u}{U} - \frac{1}{1-\phi} = a^2\nabla^2 f. \tag{6}$$

Note that the Laplacian operator is taken in the x_1–x_2 plane.

The present analysis is restricted to the case of non-adsorbing, non-reacting tube walls. The positions of the center of N tubes will be denoted by $\mathbf{x}^{\alpha}$, $\alpha = 1, 2, \ldots, N$. These centers lie within a unit cell of a periodic array. The boundary conditions for the concentration are therefore spatial periodicity and the vanishing normal component of ∇f at the surface of the tubes

$$\mathbf{n}\cdot\nabla f = 0 \quad \text{at } |\mathbf{x} - \mathbf{x}^{\alpha}| = 1. \tag{7}$$

Averaging Eq. (1) over the shell side after substituting for c from Eq. (5) and recasting the resulting expression in the form given by Eq. (3) we obtain the following expression for the Taylor dispersion coefficient:

$$\frac{D_{\mathrm{T}}}{D_{\mathrm{M}}} = 1 + \lambda Pe^2, \quad \lambda = \frac{1}{1-\phi}\left[\langle f\rangle_{\mathrm{s}} - \frac{\langle uf\rangle_{\mathrm{s}}}{U}\right], \tag{8}$$

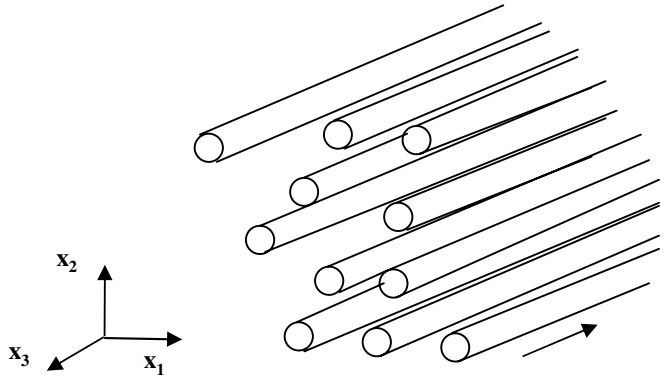

Fig. 1a. Schematic diagram of shell-and-tube configuration.

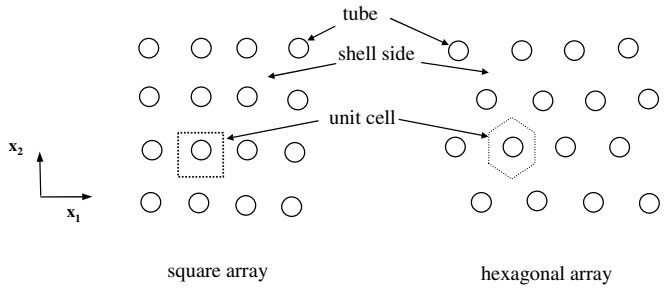

Fig. 1b. Periodic arrays (square array and hexagonal array) of tubes.

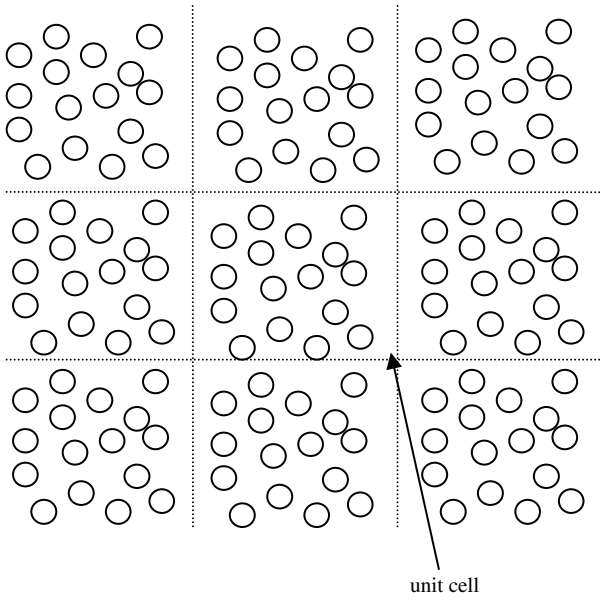

Fig. 1c. Random arrays of tubes.

where $Pe = aU/D_M$ is the Peclet number. And $\langle f\rangle_s$ and $\langle uf\rangle_s$ are defined by

$$\langle f\rangle_s = \frac{1}{(1-\phi)\tau}\int_{A_s} f\,dA, \tag{9}$$

$$\langle uf\rangle_s = \frac{1}{\tau}\int_{A_s} uf\,dA. \tag{10}$$

The method of multipole expansion is used for determining the velocity and concentration fields. The method uses periodic fundamental singular solutions of Laplace and bi-harmonic equations and their derivatives to construct velocity and concentration fields. We shall describe here in more detail the procedure for determining the velocity field that follows the analysis presented in Sangani and Yao [8]. The shell side fluid velocity satisfies

$$\nabla^2 u = G, \tag{11}$$

where G is the pressure gradient non-dimensionalized by $\mu U/a^2$. A multipole expansion expression for the velocity field is given by [8]

$$u = U_0 + \sum_{\alpha=1}^{N}\sum_{n=0}^{\infty}[A_n^\alpha \partial_1^n + \widetilde{A}_n^\alpha \partial_1^{n-1}\partial_2]S_1(\mathbf{x}-\mathbf{x}^\alpha), \tag{12}$$

where A_n^α and $\widetilde{A}_n^\alpha$ are the 2^n-multipoles induced by the presence of tube α, $\widetilde{A}_0 \equiv 0$, and $\partial_k^n = (\partial^n/\partial x_k^n)(k = 1, 2)$ is a short-hand notation for the nth order partial derivative with respect to x_k. The function S_1 is a spatially periodic function satisfying [9]

$$\nabla^2 S_1(\mathbf{x}) = 4\pi\left[\frac{1}{\tau} - \sum_{\mathbf{x}_L}\delta(\mathbf{x}-\mathbf{x}_L)\right]. \tag{13}$$

In the above expression, $\mathbf{x}_L$ are the coordinates of the lattice points of the array and δ is the Dirac's delta function. In addition to the above differential equation we require that the integral of S_1 over the unit cell be zero. A Fourier series representation of S_1 and an efficient technique based on Ewald summation for evaluating S_1 are described by Hasimoto [9]. Substituting Eq. (12) into Eq. (11), and making use of Eq. (13), we find that the non-dimensional pressure gradient is related to the sum of monopoles:

$$G = \frac{4\pi}{\tau}\sum_{\alpha=1}^{N} A_0^\alpha = 4\phi\langle A_0\rangle, \tag{14}$$

where $\langle A_0\rangle$ is the average monopole. The multipoles A_n^α and $\widetilde{A}_n^\alpha$ and the constant U_0 in Eq. (12) are to be determined from the no-slip boundary condition $u = 0$ on the surface of the tubes and Eq. (11), which states that the non-dimensional superficial velocity is unity. For this purpose it is convenient to re-expand u around the center of each tube. For example, u is expanded near tube α as

$$u = \sum_{n=0}^{\infty}[u_n^\alpha(r)\cos n\theta + \tilde{u}_n^\alpha(r)\sin n\theta] \tag{15}$$

with

$$u_n^\alpha(r) = a_n^\alpha r^{-n} + e_n^\alpha r^n \quad \text{for } n \geqslant 1,$$
$$u_0^\alpha(r) = a_0^\alpha \log r + e_0^\alpha + Gr^2/4, \tag{16}$$

where $r = |\mathbf{x} - \mathbf{x}^\alpha|$. The terms singular at $r = 0$ in the above expression arise from the singular part of S_1 at $r = 0$. Noting that S_1 behaves as $-2\log r$ as $r \to 0$ (Hasimoto [9]), and using the formulas for the derivatives of $\log r$ given in Appendix A, we obtain

$$a_0^\alpha = -2A_0^\alpha, \quad a_n^\alpha = 2(-1)^n(n-1)!A_n^\alpha \quad \text{for } n \geqslant 1. \tag{17}$$

The coefficients $\widetilde{A}_n^\alpha$ are similarly related to $\tilde{a}_n^\alpha$. The coefficients of the regular terms, such as e_n^α, are related to the derivatives of the regular part of u at $\mathbf{x} = \mathbf{x}^\alpha$ [8]. For example

$$e_n^\alpha = \frac{1}{n!}[\partial_1^n - \xi_n\partial_1^{n-2}\nabla^2]u^r(\mathbf{x}^\alpha), \tag{18}$$

$$\tilde{e}_n^\alpha = \frac{1}{n!}[\partial_1^{n-1}\partial_2 - \tilde{\xi}_n\partial_1^{n-3}\partial_2\nabla^2]u^r(\mathbf{x}^\alpha), \tag{19}$$

where $\xi_n = n/4$ for $n \geqslant 2$, $\tilde{\xi}_n = (n-2)/4$ for $n \geqslant 3$, and $\xi_0 = \xi_1 = \tilde{\xi}_1 = \tilde{\xi}_2 = 0$. In Eqs. (18) and (19), u^r denotes the regular part u obtained by removing the singular part, $-2\log r$, from $S_1(\mathbf{x} - \mathbf{x}^\alpha)$.

To determine the relation between U_0 in Eq. (12) and the superficial velocity we must integrate u over the area A_s occupied by the shell side fluid. Since the integrals of S_1 and its derivatives over the unit cell vanish, it is easier to evaluate the integral of u over A_s by integrating Eq. (12) over the unit cell and subtracting from it the integral of u inside the tubes. With the non-dimensional superficial velocity taken as unity, the above procedure yields

$$1 = U_0 - \frac{1}{\tau}\sum_{\alpha=1}^{N}\int_{r=0}^{1}\int_{\theta=0}^{2\pi} u^\alpha(r,\theta)r\,dr\,d\theta. \tag{20}$$

Care must be taken in carrying out above integration to account for the singular nature of u^α at $\mathbf{x} = \mathbf{x}^\alpha$. Upon carrying out integration, we obtain

$$U_0 = 1 + \phi(1-\phi/2)\langle A_0\rangle + 2\phi\langle A_2\rangle. \tag{21}$$

The no-slip boundary condition on the surface of the tube, together with the orthogonality of trigonometric functions, requires that

$$u_n^\alpha(1) = \tilde{u}_n^\alpha(1) = 0. \tag{22}$$

Substituting for a_n^α and e_n^α from Eqs. (17) and (18) into expressions for u_n^α and applying Eq. (22) we obtain a set of linear equations in the multipole coefficients A_n^α. This set is truncated by retaining only the terms with $n \leqslant N_s$ to yield a total of $2N_s + 1$ equations in the same number of unknowns, solving which yields the velocity of the fluid on the shell side.

The concentration of the fluid on the shell side is determined in a similar manner. A formal solution of Eq. (3) that is spatially periodic is given by

$$f(\mathbf{x}) = \sum_{\alpha=1}^{N}\sum_{n=0}^{\infty}[B_n^\alpha \partial_1^n + \widetilde{B}_n^\alpha \partial_1^{n-1}\partial_2]S_1(\mathbf{x}-\mathbf{x}^\alpha) + [A_n^\alpha \partial_1^n + \widetilde{A}_n^\alpha \partial_1^{n-1}\partial_2]S_2(\mathbf{x}-\mathbf{x}^\alpha), \tag{23}$$

where the spatially periodic function S_2 satisfies

$$\nabla^2 S_2 = S_1. \tag{24}$$

As shown by Hasimoto [9]

$$S_m(\mathbf{x}) = \frac{1}{\pi\tau(-4\pi^2)^{m-1}}\sum_{\mathbf{k}\neq\mathbf{0}} k^{-2m}\exp(2\pi i\mathbf{k}\cdot\mathbf{x}), \tag{25}$$

where the summation is over all reciprocal lattice vectors except $\mathbf{k}=\mathbf{0}$. As mentioned earlier, Hasimoto [9] has described a method for evaluating these functions using the Ewald summation technique.

Substituting for f and u_s from Eqs. (23) and (12) into Eq. (6) and using Eqs. (13) and (24), we find that, in order for Eq. (23) to be the solution for f, we must have

$$\frac{4\pi}{\tau}\sum_{\alpha=1}^{N} B_0^\alpha = U_0 - \frac{1}{1-\phi}. \tag{26}$$

To determine the multipoles B_n, we expand f near the center of each tube. Near tube α

$$f(\mathbf{x}) = \sum_{n=0}^{\infty} f_n^\alpha(r)\cos n\theta + \tilde{f}_n^\alpha(r)\sin n\theta \tag{27}$$

with

$$f_0^\alpha = -\frac{1}{4}r^2(1-\log r)a_0^\alpha + \frac{r^2}{4}e_0^\alpha + b_0^\alpha \log r + g_0 + \frac{r^4}{64}G - \frac{1}{1-\phi}\frac{r^2}{4}, \tag{28}$$

$$f_1^\alpha = \frac{1}{2}r\left(\log r - \frac{1}{2}\right)a_1^\alpha + \frac{r^3}{8}e_1^\alpha + b_1^\alpha r^{-1} + g_1^\alpha r, \tag{29}$$

$$f_n^\alpha = \frac{r^{2-n}}{4(1-n)}a_n^\alpha + \frac{r^{n+1}}{4(n+1)}e_n^\alpha + b_n^\alpha r^{-n} + g_n^\alpha r^n \quad \text{for } n \geqslant 2, \tag{30}$$

and similar expressions for $\tilde{f}_n^\alpha$. Once again, the coefficients of the singular terms, e.g., b_n^α, can be related to the multipoles induced by tube α (i.e., A_n^α and B_n^α) and the coefficients of regular terms, g_n^α can be related to the derivatives of the regular part of f at $\mathbf{x}=\mathbf{x}^\alpha$. The results are given in Appendix A. The condition of vanishing flux integrated over the surface of the tube yields

$$B_0^\alpha = \frac{1}{4}A_0^\alpha - \frac{1}{32}G + \frac{1}{4\phi} - \frac{1}{2}A_2^\alpha - \frac{1}{4(1-\phi)}. \tag{31}$$

Thus, we see the monopole induced is not an unknown. On noting that U_0 is given by Eq. (21), we see that the condition Eq. (26) is automatically satisfied.

The average concentration of the shell side fluid is determined from integrating f given by Eq. (23) over the entire unit cell and subtracting from it the integrals over the area occupied by the tubes. The latter are evaluated using the local expansion near each tube (cf. Eq. (27)). The resulting expression is

$$\langle f\rangle_s = \frac{3\phi}{8(1-\phi)} - \frac{\phi\langle g_0\rangle}{1-\phi} + \frac{\phi}{96}\frac{(27-11\phi)}{1-\phi}\langle a_0\rangle + \frac{\phi}{1-\phi}\langle b_2\rangle - \frac{\phi}{24(1-\phi)}\langle a_4\rangle. \tag{32}$$

Here, $\langle g_0\rangle$, $\langle a_0\rangle$, $\langle b_2\rangle$, and $\langle a_4\rangle$ are averages of each coefficient defined in the same manner as $\langle A_0\rangle$ in Eq. (14).

For determining $\langle uf\rangle_s$, we need to integrate the product uf over the area occupied by the shell side fluid. This is difficult because it would require evaluating S_1, S_2, and their derivatives at many points outside the tubes. It is more efficient instead to solve for an auxiliary function ψ defined by

$$\nabla^2\psi = f, \quad \psi = 0 \quad \text{at } |\mathbf{x}-\mathbf{x}^\alpha| = 1. \tag{33}$$

Substituting for f from Eq. (33) into Eq. (10) and using Green's theorem we obtain

$$\tau\langle uf\rangle_s = \int_{A_s} uf\,\mathrm{d}A = \int_{A_s} u\nabla^2\psi\,\mathrm{d}A = \int_{A_s}\psi\nabla^2 u\,\mathrm{d}A + \int_{\partial A_s}(u\nabla\psi - \psi\nabla u)\cdot\mathbf{n}\,\mathrm{d}l. \tag{34}$$

The integral over ∂A_s, which consists of the unit cell boundary and the surface of the tubes, vanishes owing to the boundary condition $u=\psi=0$ on the tube surface and the spatial periodicity of ψ and u. On using Eq. (11) we obtain

$$\langle uf\rangle_s = \frac{G}{\tau}\int_{A_s}\psi\,\mathrm{d}A. \tag{35}$$

A formal expression for ψ can be written in the same way as for u and f:

$$\psi(\mathbf{x}) = \psi_0 + \sum_{\alpha=1}^{N}\sum_{n=0}^{\infty}[C_n^\alpha\partial_1^n + \widetilde{C}_n^\alpha\partial_1^{n-1}\partial_2]S_1 + [B_n^\alpha\partial_1^n + \widetilde{B}_n^\alpha\partial_1^{n-1}\partial_2]S_2 + [A_n^\alpha\partial_1^n + \widetilde{A}_n^\alpha\partial_1^{n-1}\partial_2]S_3, \tag{36}$$

where S_1, S_2 and S_3, and their derivatives, are to be evaluated at $\mathbf{x}-\mathbf{x}^\alpha$, and $\nabla^2 S_3 = S_2$. Expression Eq. (25) with $m=3$ can be used to evaluate S_3. The coefficients ψ_0, C_n and $\widetilde{C}_n$ are to be evaluated from the boundary condition $\psi=0$ on the surface of the tubes. Finally, since $\nabla^2 S_1 = 4\pi/\tau$ at all points outside the tubes, we require that

$$\sum_{\alpha=1}^{N} C_0^\alpha = 0. \tag{37}$$

To determine the coefficients $\widetilde{C}_n^\alpha$, we expand ψ near the surface of each tube as

$$\psi = \sum_{n=0}^{\infty}\psi_n(r)\cos n\theta + \tilde{\psi}_n(r)\sin n\theta \tag{38}$$

with

$$\psi_n = \psi_n^r + \psi_n^s, \tag{39}$$

$$\psi_n^r = h_n r^n + \frac{g_n}{4(1+n)}r^{n+2} + \frac{e_n}{32(n+1)(n+2)}r^{n+4} + \frac{G}{32\cdot 12\cdot 6}r^6\delta_{n0} - \frac{\delta_{n0}}{64(1-\phi)}r^4 \quad \text{for } n \geqslant 0. \tag{40}$$

For the purpose of applying boundary condition at $r = 1$, we evaluate ψ_n^s at $r = 1$ using

$$\psi_n^s = \beta_1 A_n + \beta_2 A_{n+2} + \beta_3 A_{n+4} + \beta_4 B_n + \beta_5 B_{n+2} + \beta_6 C_n, \tag{41}$$

where

$$\begin{aligned}
&\beta_1 = \frac{(-1)^n (n-3)!}{16}, \quad \beta_2 = \frac{(-1)^{n+1}(n-2)!(n+2)}{8},\\
&\beta_3 = \frac{(-1)^n n!(n+3)(n+4)}{16n},\\
&\beta_4 = \frac{(-1)^{n+1}(n-2)!}{8}, \quad \beta_5 = \frac{(-1)^{n+1} n!(n+2)}{2n},\\
&\beta_6 = 2(-1)^n (n-1)!\\
&\beta_1 = 3/64, \quad \beta_2 = 1/4, \quad \beta_4 = 1/2, \quad \beta_3 = \beta_5 = \beta_6 = 0 \quad \text{for } n = 0,\\
&\beta_1 = 5/32, \quad \beta_2 = 3/8, \quad \beta_4 = 1/2 \quad \text{for } n = 1,\\
&\beta_1 = 3/32 \quad \text{for } n = 2.
\end{aligned} \tag{42}$$

Now the integral of ψ over the area occupied by the shell side fluid can be determined by integrating ψ given by Eq. (36) over the unit cell first and then subtracting from it the integrals inside the tubes using the expression Eq. (38) for ψ near each tube. The final result for the mixing-cup based concentration difference is

$$\begin{aligned}
\langle uf \rangle_s = -G\phi \Bigg[&\frac{5}{32\cdot 9}\langle A_0 \rangle + \frac{5}{32}\langle A_2 \rangle + \frac{3}{8}\langle A_4 \rangle + \frac{5}{4}\langle A_6 \rangle + \frac{5}{16}\langle B_0 \rangle \\
&+ \frac{\langle B_2 \rangle}{2} - \frac{3}{2}\langle B_4 \rangle + \langle C_0 \rangle - 2\langle C_2 \rangle + \langle h_0 \rangle + \frac{\langle g_0 \rangle}{8} \\
&+ \frac{1}{32\cdot 6}\left(\langle e_0 \rangle - \frac{1}{1-\phi} \right) + \frac{G}{32\cdot 12\cdot 8\cdot 6} - \frac{\psi_0}{\phi} \Bigg].
\end{aligned} \tag{43}$$

Here, the averages of multipoles and coefficients are also defined in the same manner as $\langle A_0 \rangle$ in Eq. (14).

3. Results and discussion

3.1. Periodic arrays

The simulation results for the coefficient λ as a function of ϕ for square and hexagonal arrays are given in Fig. 3. It is found that the coefficient λ shows minimum value around $\phi = 0.2$ and 0.4 for square and hexagonal array, respectively. This behavior is due to the difference in dependency of $\langle f \rangle_s$ and $\langle uf \rangle_s$ on ϕ. Since both velocity and concentration field are disturbed due to the presence of tube and the magnitude of the disturbance increases with ϕ, it is easily expected that $\langle uf \rangle_s$ is more affected by the disturbance than $\langle f \rangle_s$ and thus the difference between the two terms become large. It is also noted that the dispersion in square array is larger than that in hexagonal array.

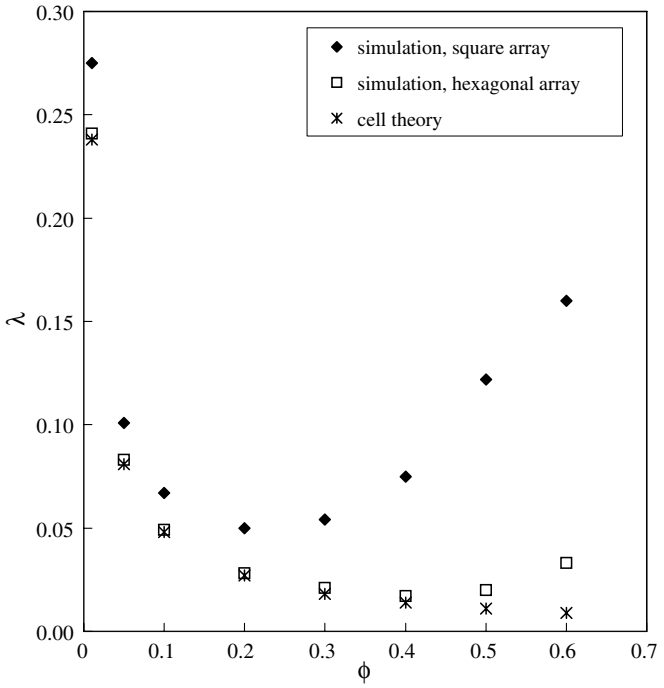

Fig. 2. The coefficient λ for periodic arrays as function of ϕ.

The results of exact calculations are compared with the predictions obtained using a cell theory [10] which is more appropriate for periodic arrays than effective-medium theory. In this theory, the periodic unit cell is replaced by a fluid cell of outer radius $R_c = \phi^{-1/2}$ and inner radius unity. (Fig. 2) The fluid velocity is given by

$$u = -2A_0 \log r + \frac{G}{4} r^2 + e_0. \tag{44}$$

The constants are determined using Eq. (14) and the boundary conditions $u = 0$ at $r = 1$ and $\partial u/\partial r = 0$ at $r = R_c$, and the condition that the average velocity of the fluid in the cell equals $1/(1-\phi)$. This yields

$$-\frac{1}{A_0} = \log R_c^2 - \frac{3}{2} + \frac{2}{R_c^2} - \frac{1}{2R_c^4}. \tag{45}$$

Similarly from Eq. (6) the concentration for the shell side fluid is given by

$$\begin{aligned}
f = A_0 \left[\frac{1}{2} r^2 (1 - \log r) + \frac{1}{R_c^2}\left(\frac{r^4}{16} - \frac{r^2}{4} \right) \right] - 2B_0 \log r \\
- \frac{r^2}{4(1-\phi)} \quad \text{for } r > 1.
\end{aligned} \tag{46}$$

The constant B_0 is determined using the conditions of no flux at $r = 1$ and at $r = R_c$. The average concentrations of the fluids, and hence the Taylor dispersion coefficients, can be determined once this constant is determined. The results are given below.

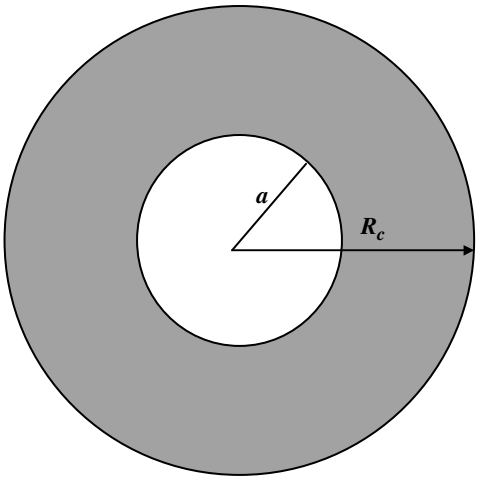

Fig. 3. Cell model.

$$\langle f\rangle_s = \frac{2}{R_c^2-1}\left\{A_0\left(\frac{R_c^4}{6}-\frac{R_c^4\log R_c}{8}-\frac{R_c^2}{16}-\frac{5}{48}\right) + B_0\left(-R_c^2\log R_c+\frac{R_c^2-1}{2}\right)-\frac{R_c^4-1}{16(1-\phi)}\right\}, \tag{47}$$

$$\begin{aligned}\langle uf\rangle_s = \frac{2}{R_c^2}\Bigg[A_0^2\Bigg\{&\left(-\frac{R_c^4\log R}{4}+\frac{1}{16}(R_c^4-1)\right)\left(1-\frac{1}{R_c^2}\right)\\ &+\frac{5}{48}\left(-R_c^2\log R_c+\frac{1}{6}\left(R_c^4-\frac{1}{R_c^2}\right)\right)\\ &+\frac{R_c^4}{8}\log R_c(2\log R_c-1)+\frac{1}{32}(R_c^4-1)\\ &+\frac{1}{2R_c^2}\left(\frac{R_c^6}{6}-\frac{R_c^4}{4}+\frac{1}{12}\right)+\frac{1}{R_c^4}\left(\frac{R_c^8}{128}-\frac{5R_c^6}{96}+\frac{R_c^4}{16}-\frac{7}{384}\right)\Bigg\}\\ &+A_0B_0\Bigg\{2R_c^2\left((\log R_c)^2-\log R_c+\frac{1}{2}\right)-1\\ &-\frac{2}{R_c^2}\left(\frac{R_c^4}{4}\log R_c-\frac{R_c^4-1}{16}-\frac{R_c^2}{2}\log R_c+\frac{R_c^2-1}{4}\right)\Bigg\}\\ &-\frac{A_0}{4(1-\phi)}\Bigg\{-\frac{1}{2}R_c^4\log R_c+\frac{1}{8}(R_c^4-1)\\ &+\frac{1}{R_c^2}\left(\frac{R_c^6}{6}-\frac{R_c^4}{4}+\frac{1}{12}\right)\Bigg\}\Bigg].\end{aligned} \tag{48}$$

The predictions obtained using the cell theory are shown in Fig. 3. It is seen that the cell theory is more accurate for hexagonal arrays as might be expected based on the observation that a hexagonal cell is closer to the circular cell used in the theory than a square cell.

3.2. Random arrays

Now, the more interesting case of random arrays is considered. Fig. 4 shows the coefficient λ as functions of N, the number of tubes per unit cell, for $\phi = 0.1$. The results were obtained by averaging shell side concentration difference over 100 hard-disk configurations for each N. A molecular dynamics code was used for generating hard-disk random configurations. We see that the coefficient λ increases logarithmically with N at large N. The solid lines in this Fig. 4 indicate the slopes predicted by the theory to be described next.

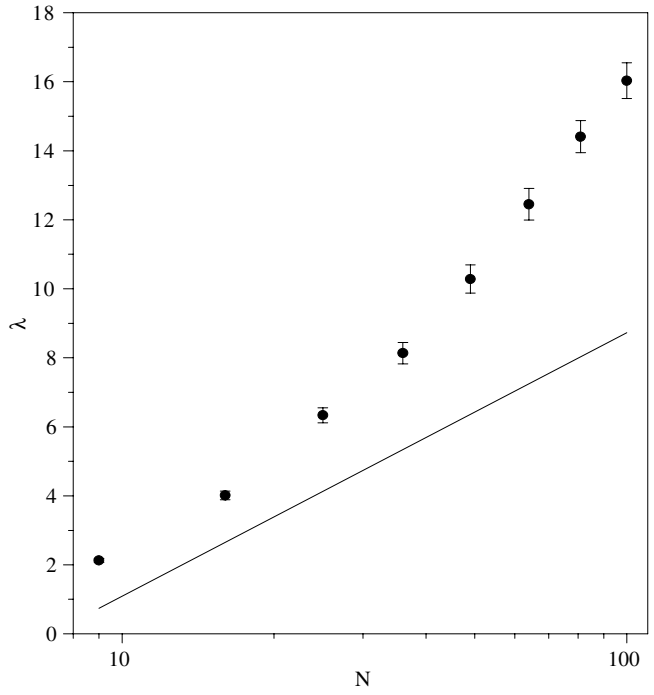

Fig. 4. The logarithmic divergence of the coefficient λ with the number of tubes N, at $\phi = 0.1$.

As mentioned in the Introduction the logarithmic divergence arises due to the fact that the fundamental solution of Laplace equation in a two-dimensional space is $\log r$. The tube side fluid acts as a source of solute while the shell side as a sink. The present study will show that there is a net source due to the presence of each tube, and this would imply that the concentration disturbance caused by a tube would grow logarithmically. To show this let us begin by deriving the equation for the conditionally-averaged concentration, i.e., the ensemble-averaged solute concentration subject to a condition that a tube is present with its center fixed at origin.

The equation governing the conditionally-averaged concentration outside the tube is slightly complicated since a given point may lie inside another tube or outside all the tubes. Let χ be an indicator function whose value at a given point is unity if it lies inside a tube and zero otherwise. The conditionally-averaged source density $\langle\varphi\rangle_1$ then equals

$$\langle(1-\chi)\nabla^2 f\rangle_1(\mathbf{r}|\mathbf{0}) = \langle\varphi\rangle_1 = \langle(1-\chi)(u-(1-\phi)^{-1})\rangle_1(\mathbf{r}|\mathbf{0}), \tag{49}$$

where $\langle f\rangle_1$ is the conditionally-averaged concentration. The apparent source due to the presence of tube at the origin as seen from a distance R is therefore given by

$$J_{ap} = 2\pi\int_0^R \langle-(1-\chi)(u-(1-\phi)^{-1})\rangle_1(\mathbf{r}|\mathbf{0})r\,dr. \tag{50}$$

The above source must equal the net outward solute transfer from the surface $r = R$. At large r, the source density vanishes since the conditional averages converge

to the unconditional averages and $\langle(1-\chi)u\rangle_0 = \langle(1-\chi)(1-\phi)^{-1}\rangle_0 = 1$. The integrand in the last integral in Eq. (50) therefore vanishes at large r and one may substitute $R=\infty$ for the purpose of evaluating the total apparent source due to the presence of a tube at origin. Since $\langle f\rangle_1(\mathbf{r}|\mathbf{0})$ must be function of r only for a random isotropic medium, and must satisfy Laplace equation at large r where the source density $\langle\varphi\rangle_1$ vanishes, we must have that for large r

$$\langle f\rangle_1(\mathbf{r}|\mathbf{0}) \to -J_{\mathrm{ap}}\log r/(2\pi k^*) + \text{const.} \tag{51}$$

Here, k^* is the effective diffusivity at large r satisfying $\langle\mathbf{j}\rangle_1 = -k^*\nabla\langle c\rangle_1$, where $\langle c\rangle_1$ and $\langle\mathbf{j}\rangle_1$ are, respectively, the conditionally-averaged concentration and flux. The problem of predicting the effective diffusivity k^* of a medium containing disks of diffusivity κ_c randomly dispersed in a medium of unit diffusivity has been examined by a number of investigators in the past including Sangani and Yao [11] who presented results for k^* as a function of κ_c and ϕ. In the present study, k^* corresponds to the value when κ_c vanishes. The behavior of $\langle f\rangle_1$ as predicted by Eq. (51) is valid for r large compared with unity (the tube radius) but small compared with the unit cell size, i.e., for $1 \ll r \ll h$. On the unit cell length scale $\langle f\rangle_1$ must, of course, satisfy the periodicity requirement.

We analyze the problem using the method of matched asymptotic expansions with Eq. (51) representing the behavior in the inner region, $r \ll h$. In the outer region, valid for $r = \mathrm{O}(h)$, $\langle f\rangle_1$ must satisfy Laplace equation to leading order, must be spatially periodic, and must match with Eq. (51) as $r \to 0$. These conditions are satisfied by

$$\langle f\rangle_1(\mathbf{r}|\mathbf{0}) \to -J_{\mathrm{ap}}/(4\pi k^*)S_1(\mathbf{r}) + \text{const.} \tag{52}$$

The constants in Eqs. (51) and (52) need not be equal. It may be noted that the Laplacian of $\langle f\rangle_1$ as given by Eq. (52) is not exactly zero since $\nabla^2 S_1 = 4\pi\tau$. Thus the apparent source at the center of the tube is balanced by a uniform sink of strength J_{ap}/τ distributed throughout the unit cell. This sink strength, being $\mathrm{O}(h^{-2})$, does not affect the leading order behavior in the inner region.

Now using the fact that $S_1 \to 2\log(h/r) + \mathrm{O}(1)$ as $r \to 0$, and noting that $h^2 = \pi N/\phi$ it is easy to show that

$$\langle f\rangle_1(\mathbf{r}|\mathbf{0}) \to B\log N + \mathrm{O}(1) \tag{53}$$

with

$$B = J_{\mathrm{ap}}/(2\pi k^*). \tag{54}$$

To determine the constant B we must evaluate the source density $\langle\varphi\rangle_1$ in Eq. (49) and integrate it over the space outside the fixed tube. The first term on the right-hand side in Eq. (49) equals the conditionally-averaged velocity in a random array of fixed disks

$$\langle(1-\chi)u\rangle_1(\mathbf{r}|\mathbf{0}) = \langle u\rangle_1(\mathbf{r}|\mathbf{0}), \tag{55}$$

where u denotes the velocity field in a fixed bed of disks with $u = u_s$ for $\chi = 0$ and $u = 0$ for $\chi = 1$.

To determine the conditionally-averaged velocity in a fixed bed of disks, we multiply the momentum equation (11) with the fluid indicator function $1-\chi$ and ensemble average the resulting expression with a disk fixed at origin.

$$\langle(1-\chi)\nabla^2 u\rangle_1 = G\langle 1-\chi\rangle_1. \tag{56}$$

Inside the disks the velocity is zero and hence

$$\langle u\rangle_1 = \langle(1-\chi)u\rangle_1. \tag{57}$$

Taking Laplacian of the above equation we obtain

$$\begin{aligned}\nabla^2\langle u\rangle_1 &= \nabla\cdot\langle(1-\chi)\nabla u\rangle_1 - \nabla\cdot\langle u\nabla\chi\rangle_1 \\ &= \langle(1-\chi)\nabla^2 u\rangle_1 - \langle\nabla\chi\cdot\nabla u\rangle_1.\end{aligned} \tag{58}$$

Note that the second term on the right-hand side of the first equality in the above equation vanishes owing to the no-slip boundary condition. Since $\nabla\chi$ equals the unit normal vector pointing into the disk multiplied by a delta function centered at the disk circumference, the last term on the extreme right side of the above equation is given by

$$-\langle\nabla\chi\cdot\nabla u\rangle_1(\mathbf{r}|\mathbf{0}) = \int_{|\mathbf{r}-\mathbf{r}'|=1} P(\mathbf{r}'|\mathbf{0})\mathbf{n}\cdot\nabla\langle u\rangle_2(\mathbf{r}|\mathbf{0},\mathbf{r}')\,\mathrm{d}\mathbf{r}'. \tag{59}$$

The integral in the above equation can be expressed in terms of an integral on a particle centered at $\mathbf{r}$ by use of a Taylor series expansion to yield

$$\begin{aligned}-\langle\nabla\chi\cdot\nabla u\rangle_1 = P(\mathbf{r}|\mathbf{0})&\int_{|\mathbf{r}-\mathbf{r}'|=1}\mathbf{n}\cdot\nabla\langle u\rangle_2(\mathbf{r}'|\mathbf{r},\mathbf{0})\,\mathrm{d}\mathbf{r}' \\ &-\nabla\cdot\left[P(\mathbf{r}'|\mathbf{0})\int_{|\mathbf{r}-\mathbf{r}'|=1}(\mathbf{r}-\mathbf{r}')\mathbf{n}\cdot\nabla\langle u\rangle_2(\mathbf{r}'|\mathbf{r},\mathbf{0})\,\mathrm{d}\mathbf{r}'\right] \\ &+\ldots\end{aligned} \tag{60}$$

The first term on the right-hand side of the above expression can be evaluated from the local expansion of the velocity field near a representative tube α (cf. Eq. (15)) which shows the integral to equal $\pi G + 4\pi A_0^{\alpha}$. The second term is related to the stresslet induced by the presence of the disk and contributes to the effective viscosity of the medium. Ignoring the higher-order terms in Eq. (60), and combining Eqs. (56) and (58), we obtain

$$\nabla\cdot\mu_{\mathrm{B}}(r)\nabla\langle u\rangle_1 = G + 4\pi n g(r)\langle A_0\rangle_2(\mathbf{r}|\mathbf{r},\mathbf{0}), \tag{61}$$

where μ_{B} is the Brinkman viscosity and $g(r)$ is the radial distribution function defined by $P(\mathbf{r}|\mathbf{0}) = ng(r)$, n being the number density of tubes. The Brinkman viscosity is defined via the closure

$$\begin{aligned}\mu_{\mathrm{B}}(r)\nabla\langle u\rangle_1 = \nabla\langle u\rangle_1(\mathbf{r}|\mathbf{0}) + P(\mathbf{r}|\mathbf{0})&\int_{|\mathbf{r}-\mathbf{r}'|=1}(\mathbf{r}'-\mathbf{r})\mathbf{n} \\ &\cdot\nabla\langle u\rangle_2(\mathbf{r}'|\mathbf{r},\mathbf{0})\,\mathrm{d}\mathbf{r}'.\end{aligned} \tag{62}$$

The non-dimensional pressure gradient G is related to the unconditionally-averaged velocity and monopole by $G = -4\pi n\langle u\rangle_0\langle A_0\rangle_0 \equiv \kappa^2\langle u\rangle_0$ (cf. Eq. (14)).

To make further progress in determining the conditionally-averaged velocity we employ an effective-medium

approximation in which a simple, single disk model is used for determining the conditionally-averaged velocity field. Since the disks are non-overlapping, there is a net depletion in the number density of disks in the immediate vicinity of a disk. To account for this we assume an exclusion region around the fixed disk at origin for $1 < r < R$. The conditionally-averaged velocity satisfies the equations of motion for a single-phase flow (cf. Eq. (11)) in this exclusion region. Outside this region the fluid-disk medium is replaced by a medium whose properties are consistent with the average properties and average equations of motion for flow through fixed bed of disks. (Fig. 5) The radius R is chosen so that the exclusion area around a fixed disk equals that in the actual bed. Since the depletion of number density near the disk equals $n - P(\mathbf{r}|0)$, we require that

$$\pi R^2 = \frac{1}{n}\int_{r>0} [n - P(\mathbf{r}|\mathbf{0})]\,\mathrm{d}A_r. \tag{63}$$

The quantity on the right-hand side can be expressed in terms of zero wavenumber limit of the structure factor $S(\mathbf{0})$ to yield

$$\phi R^2 = 1 - S(\mathbf{0}), \tag{64}$$

where the use has been made of the relation $\phi = n\pi$. The above choice for the exclusion radius R was made by Dodd et al. [12] who showed that the effective-medium approximation based on this value of R agrees very well with the results of rigorous computations for the mobility of integral membrane proteins in bilipid membranes, modeled as suspensions of disks. Subsequently, Wang and Sangani [3], Sangani and Mo [13], and Spelt et al. [14] have used similar expressions to study a variety of problems in suspensions of disks and spheres. The computational results presented in Fig. 6 corresponded to hard-disk random configurations. $S(\mathbf{0})$ for these configurations can be evaluated using [15]

$$S(\mathbf{0}) = \frac{(1 - 1.9682\phi + 0.9716\phi^2)^2}{1 + 0.0636\phi - 0.5446\phi^2 - 0.4632\phi^3 - 0.1060\phi^4 + 0.0087\phi^5}. \tag{65}$$

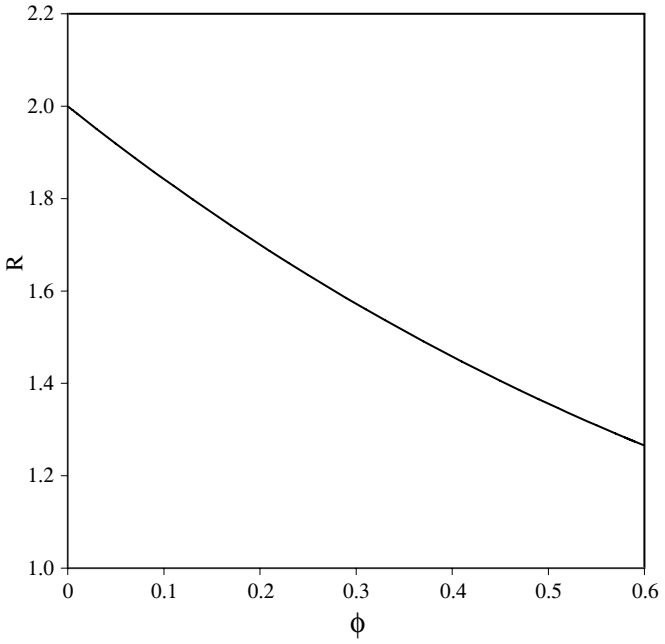

Fig. 6. The area exclusion radius R as a function of ϕ.

Note that $S(\mathbf{0}) \to 1 - 4\phi$ as $\phi \to 0$ and this yields the exclusion radius R equal to 2 in the limiting case of very dilute random suspensions. As seen in Fig. 6, the exclusion radius R decreases as ϕ increases but remains greater than unity, the radius of the disk.

Next, we introduce the following closure relation for the monopole in the effective-medium:

$$4\pi n\langle A_0\rangle_2(r) = -\kappa^2\langle u\rangle_1(r). \tag{66}$$

Finally, we take $\mu_B = 1$ for $r < R$ and a constant equal to μ^* for $r > R$. We also take $g(r) = 0$ for $r < R$ and $g(r) = 1$ for $r > R$. The conditionally-averaged velocity therefore satisfies

$$\nabla^2\langle u\rangle_1 = -\kappa^2\langle u\rangle_0 \qquad \text{for } 1 < r < R, \tag{67}$$

$$\mu^*\nabla^2\langle u\rangle_1 = \kappa^2(\langle u\rangle_1 - \langle u\rangle_0) \qquad \text{for } r > R. \tag{68}$$

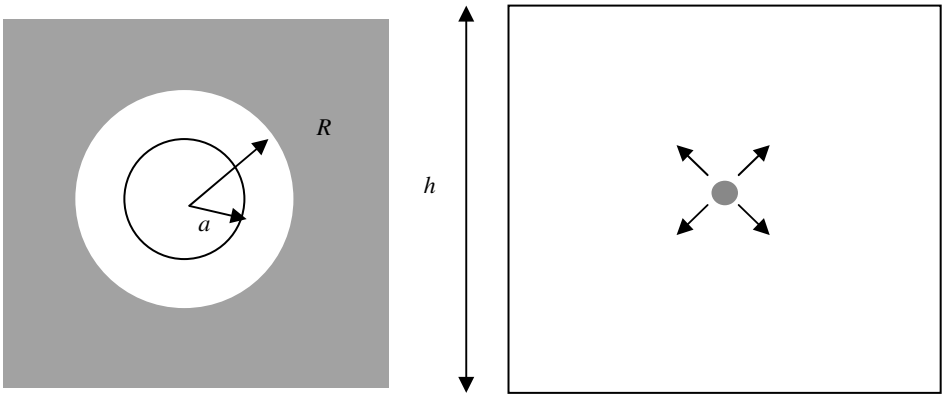

Fig. 5. Effective-medium model.

The above equations together with the boundary conditions $\langle u\rangle_1 = 0$ at $r = 1$, $\langle u\rangle_1 \to \langle u\rangle_0 = 1$ as $r \to \infty$, and the continuity of $\langle u\rangle_1$ and tangential stress at $r = R$ complete the description of the effective-medium model for determining the conditionally-averaged velocity. The above equations can be solved readily to yield

$$\langle u\rangle_1 = \begin{cases} \kappa^2(1-r^2)/4 - 2A_0 \log r & \text{for } 1 < r < R, \\ 1 + \beta K_0(\kappa^* r) & \text{for } r > R \end{cases} \tag{69}$$

with $\kappa^* = \kappa/\sqrt{\mu^*}$. Here, K_0 is the modified Bessel function of zeroth order. The constants β and A_0 are to be determined using the continuity of velocity and stress at $r = R$. The Brinkman viscosity μ^* is related to the effective diffusivity in reacting media. Calculations of Sangani and Behl [16] on diffusion into a semi-infinite medium of reacting spherical traps seem to indicate that the diffusivity of reacting media is close to the diffusivity of the medium surrounding the traps. This is equivalent to choosing $\mu^* = 1$.

We now proceed to develop an approximate theory for the conditionally-averaged solute concentration field. Using the closure relation that relates the solute flux to concentration gradient, Eq. (49) reduces to

$$k_0 \nabla^2 \langle f\rangle_1 = \langle u\rangle_1 - \frac{\langle 1-\chi\rangle_1}{1-\phi}. \tag{70}$$

As in the case of approximation for the conditionally-averaged velocity, we take $k_0 = 1$ for $1 < r < R$ and $k_0 = k^*$ for $r > R$, where, as mentioned earlier, k^* is the effective diffusivity of a medium consisting of disks of diffusivity κ_c suspended in a medium of unit diffusivity. Numerical results for k^* as a function of κ_c and ϕ, the area fraction of the disks, have been reported by a number of investigators. We shall use the results for random arrays of disks presented by Sangani and Yao [11]. On solving Eq. (70) we obtain

$$\langle f\rangle_1 = \begin{cases} \frac{\kappa^2}{4}\left(\frac{r^2}{4} - \frac{r^4}{16}\right) + \frac{4r^2}{2}(1 - \log r) + C^* \log r + D^* & \text{for } 1 \leqslant r \leqslant R \\ \frac{\beta K_0(\kappa r)}{k^* \kappa^2} + C \log r + D & \text{for } r \gg R \end{cases} \tag{71}$$

The expression for $r > R$ applies actually to distances that are small compared with the unit cell size h. For distances comparable to h, an outer region approximation for $\langle f\rangle_1$ can be obtained by noting that, since $\langle u\rangle_1 \approx \langle u\rangle_0 = 1$ for $r = O(h)$, $\langle f\rangle_1$ satisfies the Laplace equation. It is easy to show therefore that

$$\langle f\rangle_1(\mathbf{r}) = BS_1(\mathbf{r}) + \langle f\rangle_0 \quad \text{for } r = O(h). \tag{72}$$

The unconditionally-averaged solute concentration $\langle f\rangle_0$ can be set to zero with no loss of generality. The relation between B, C and D can be determined by requiring that the above expression agrees in the limit $r/h \to 0$ with that for the inner region given by Eq. (71) as $r \to \infty$. For small r/h, S_1 for square lattice is given by

$$S_1 = -2\log(r/h) - 2.6232 + O(r/h)^2. \tag{73}$$

Matching the solution for $\langle f\rangle_1$ in the two regions therefore yields

$$\begin{aligned} C &= -2B, D = B(2\log h - 2.6232) \\ &= B(\log N - \log\phi - 1.4763). \end{aligned} \tag{74}$$

The constants B, C^*, and D^* can be determined now from the continuity of concentration and flux at $r = 1$ and $r = R$ (Appendix B).

Next, we develop an approximate theory for determining the conditionally-averaged ψ and hence the mixing-cup solute concentrations in the shell side fluid. Taking $\psi = 0$ inside the tubes and averaging the governing equations for ψ yields, as in the case of conditionally-averaged velocity, the following equation:

$$\nabla^2 \langle\psi\rangle_1 = \langle (1-\chi) f_s\rangle_1 - \langle \nabla\chi \cdot \nabla\psi\rangle_1. \tag{75}$$

The last term on the right-hand side of the above equation can be approximated through the use of a Taylor series expansion to yield

$$\langle \nabla\chi \cdot \nabla\psi\rangle_1 = ng(r) \int_{|x-x_1|=1} \mathbf{n} \cdot \nabla \langle\psi\rangle_2(\mathbf{x_1}|\mathbf{x}, \mathbf{0})\, \mathrm{d}l + \cdots. \tag{76}$$

The higher-order term in the above expression contributes a property similar to the Brinkman viscosity, which, as discussed earlier, can be taken to be unity. The integral in the above expression can be expressed alternatively using the divergence theorem as

$$\int_{|x-x_1|\leqslant 1} \nabla^2 \langle\psi^{\mathrm{ext}}\rangle_2\, \mathrm{d}A = \int_{|x-x_1|\leqslant 1} f_s^{\mathrm{ext}}\, \mathrm{d}A - 4\pi \langle C_0\rangle_2, \tag{77}$$

where ψ^{ext} and f_s^{ext} are, respectively, the analytical extensions of ψ and f_s into a tube centered at $\mathbf{x}$ and C_0 is the monopole coefficient in the expression for ψ near the surface of a tube (cf. Eq. (40)). Now using $\langle (1-\chi)\, f_s\rangle_1 = \langle f\rangle_1 - \langle \chi f_t\rangle_1$, Eq. (75) becomes

$$\nabla^2 \langle\psi\rangle_1 = \langle f\rangle_1 - 4\pi n g(r) \langle C_0\rangle_2 - ng(r) \int_{|x-x_1|\leqslant 1} f_s^{\mathrm{ext}}\, \mathrm{d}A. \tag{78}$$

Using the expression for f_s near a representative tube (cf. Eq. (27)), the above integral can be readily evaluated to yield

$$\begin{aligned} \nabla^2 \langle\psi\rangle_1 = \langle f\rangle_1 - \langle f\rangle_0 + ng(r)\frac{\pi}{16}[\langle A\rangle_2 - \langle A\rangle_0] \\ - 4\pi n g(r) \langle C_0\rangle_2, \end{aligned} \tag{79}$$

where the use has been made of Eq. (66) and $4\pi n \langle u\rangle_0 \langle A_0\rangle_0 = -\kappa^2 \langle u\rangle_0$. Now we need to specify a closure relation for $\langle C_0\rangle_2$. The condition Eq. (37) can be expressed equivalently as

$$\langle C_0\rangle + n \int_{r\geqslant 2} g(r) \langle C_0\rangle_2\, \mathrm{d}A = 0. \tag{80}$$

The average monopole $\langle C_0 \rangle$ is zero. We therefore take, analogous to the closure for the monopole $\langle A_0 \rangle$ used in the expression for the velocity field

$$4\pi n \langle C_0 \rangle_2 = -\kappa^2 (\langle \psi \rangle_1(\mathbf{r}|\mathbf{0}) - \langle \psi \rangle_0). \tag{81}$$

Substituting for $\langle C_0 \rangle_2$ from Eq. (81) into Eq. (79) and taking $g(r) = 1$ for $r > R$ and 0 for $r < R$ we obtain equations for an effective-medium approximation for $\langle \psi \rangle_1$.

In the outer region, i.e., for $r = \mathrm{O}(h)$, $\langle u \rangle_1$ approximately equals $\langle u \rangle_0$. Using Eq. (72) for $\langle f \rangle_1 - \langle f \rangle_0$, we have

$$\langle \psi \rangle_1 = \langle \psi \rangle_0 - (B/\kappa^2) S_1 \quad \text{for } r = \mathrm{O}(h). \tag{82}$$

The condition that the above expression must match with the inner region approximation for $\langle \psi \rangle_1$ for $r \ll h$ yields

$$\langle \psi \rangle_1 = \begin{cases} \frac{A_0 r^4}{64}(3 - 2\log r) + \frac{B_0 r^2}{2}(1 - \log r) - 2C_0 \log r + h_0 + \frac{g_0 r^2}{4} \\ -\frac{A_0 \phi r^4}{64} + \frac{A_0 \phi}{576} \quad \text{for } 1 \leqslant r \leqslant R, \\ \frac{B}{\kappa^2}(2\log r - \log N + \log \phi + 1.4763) - \frac{rK_1(\kappa r)}{2\kappa}\left[\frac{\beta}{k^* \kappa^2} - \frac{\beta \kappa^2}{64}\right] \\ +\gamma K_0(\kappa r) + \langle \psi \rangle_0 \quad \text{for } r \gg R. \end{cases} \tag{83}$$

The unknowns $\langle \psi \rangle_0$ and γ are determined by requiring that both $\langle \psi \rangle_1$ and its derivative are continuous at $r = R$. Then the mixing-cup solute concentration in the shell side fluid is determined using $\langle uf \rangle_s = G \langle \psi \rangle_0 = 4\pi n \kappa^2 \langle \psi \rangle_0$ (cf. Eq. (35)). Finally, the results of effective-medium approximation can be expressed as

$$\lambda = \lambda_1 \log N + \lambda_2, \tag{84}$$

where

$$\lambda_1 = 4\phi A_0 B \left(\frac{1 - R^2}{4} - \frac{1}{\kappa^2} - \frac{R}{2\kappa} \frac{K_0(\kappa R)}{K_1(\kappa R)} - \frac{1}{4A_0(1-\phi)^2} \right), \tag{85}$$

$$\lambda_2 = 1 + \frac{3\phi}{8(1-\phi)^2} - \frac{\phi}{(1-\phi)^2} D^*_{\mathrm{ex}} - \frac{\phi(27 - 11\phi)A_0}{48(1-\phi)^2} - 4\phi A_0 \psi_{0,\mathrm{ex}}. \tag{86}$$

The expressions for the constants B, $\psi_{0,\mathrm{ex}}$, and D^*_{ex} are given in Appendix B. The predictions of the coefficients λ by the effective-medium approximation are compared with the exact calculations for $\phi = 0.1$, 0.3, and 0.5 in Fig. 7. As in Fig. 4, the coefficients λ are shown to be logarithmically divergent with the number of tubes at these area fractions of tubes. We see that the approximation slightly underpredicts the coefficients λ. In addition, the coefficients λ_1 and λ_2 obtained by the numerical simulations and the effective-medium theory are plotted as functions of ϕ in Figs. 8 and 9. The filled circles in these figures are the estimates of λ_1 and λ_2 obtained by fitting the results of numerical computations of the coefficients λ as functions of N in Fig. 7. We find that the predictions of λ_1 and λ_2 as functions of ϕ by the effective-medium approximation are in qualitative agreement with the results of numerical computations.

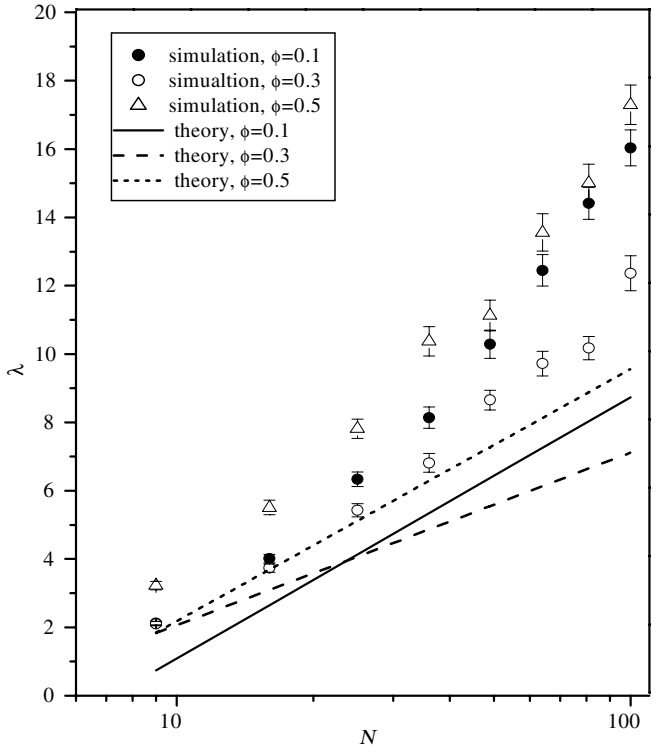

Fig. 7. λ versus N at $\phi = 0.1$, 0.3, and 0.5.

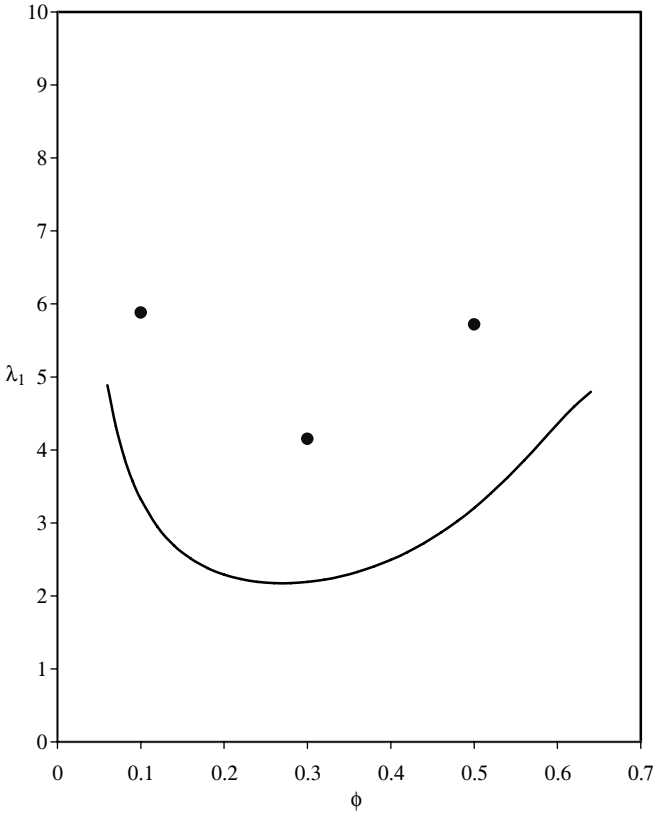

Fig. 8. λ_1 versus ϕ.

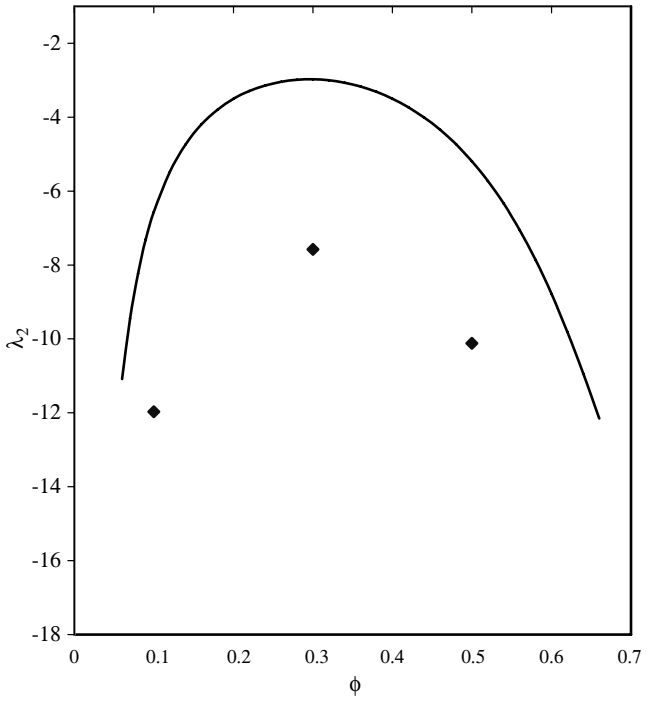

Fig. 9. λ_2 versus ϕ.

4. Conclusion

Numerical simulations have been carried out to determine shell-side Taylor dispersion coefficients for laminar, longitudinal flow along the axes of tubes for the case of non-absorbing, non-reacting tube walls. Both periodic as well as random arrays of tubes are considered. The latter is modeled by randomly placing N tubes within a unit cell of a periodic array. It is found that shell-side Taylor dispersion coefficient D_T is expressed by $D_T = D_M(1 + \lambda Pe^2)$ and the coefficient λ diverges as N increases, where D_M is the molecular diffusivity of solute on the shell side and Pe is the Peclet number given by aU/D_M with a and U being the radius of tube and the mean fluid velocity on the shell side, respectively. The coefficient λ is determined by the spatial average and the fluid velocity weighted average of the concentration of solute on the shell side. The behavior of the coefficient λ arises due to logarithmically divergent nature of concentration disturbances caused by each tube in the plane normal to the axes of the tubes. An effective-medium theory is developed for determining conditionally-averaged velocity and concentration fields and hence the shell-side Taylor dispersion coefficient. Its predictions are compared with the results of rigorous numerical computations. This comparison shows that the effective-medium theory slightly underpredicts the logarithmic dependence of the shell-side Taylor dispersion coefficients with the number of tubes. However the theoretical predictions for the coefficients of the logarithmic dependence as functions of the number of tubes are in qualitative agreement with the numerical simulation results. And the present analysis also provides the shell-side Taylor dispersion coefficients for the periodic arrays, i.e., square and hexagonal arrays, which are smaller than those for the random arrays. These simulation results are compared with a cell theory approximation for wide range of area fractions of tubes. Agreement between the cell theory and numerical results is excellent at small area fractions. At larger area fractions, the cell theory gives better estimates for hexagonal arrays due to geometrical closeness.

Acknowledgements

Author acknowledges Professor Ashok S. Sangani of Syracuse University, Syracuse, NY, USA for his suggestions.

Appendix A

Formulas for determining the coefficients of regular terms

$$g_n^\alpha = \frac{1}{n!}\partial_1^n T_s^r(\mathbf{x}^\alpha) - \frac{e_{n-2}^\alpha}{4(n-1)} - \frac{G}{64}\delta_{n4}, \tag{A1}$$

$$\tilde{g}_n^\alpha = \frac{1}{n!}\partial_1^{n-1}\partial_2 T_s^r(\mathbf{x}^\alpha) - \frac{\tilde{e}_{n-2}^\alpha}{4(n-1)}\frac{n-2}{n}, \tag{A2}$$

$$h_n^\alpha = \frac{1}{n!}\partial_1^n \psi^r(\mathbf{x}^\alpha) - \frac{g_{n-2}^\alpha}{4(n-1)} - \frac{e_{n-4}^\alpha}{32(n-2)(n-3)} + \frac{\delta_{n4}}{64(1-\phi)} - \frac{G}{32\cdot 12\cdot 6}\delta_{n6}, \tag{A3}$$

$$\tilde{h}_n^\alpha = \frac{1}{n!}\partial_1^{n-1}\partial_2 \psi^r(\mathbf{x}^\alpha) - \frac{n-2}{n}\frac{\tilde{g}_{n-2}^\alpha}{4(n-1)} - \frac{n-4}{n}\frac{\tilde{e}_{n-4}^\alpha}{32(n-2)(n-3)}. \tag{A4}$$

Appendix B

Formulas for the coefficients B, C, C^*, D, D^*, D_{ex}^*, and $\langle\psi\rangle_{0,ex}$

$$B = -\frac{C}{2}, \tag{B1}$$

$$C = \frac{R}{k^*}\left[\frac{\kappa^2}{4}\left(\frac{R}{2} - \frac{R^3}{4}\right) + \frac{A_0 R}{2}(1 - 2\log R) - \frac{R}{2(1-\phi)} + \frac{\beta}{\kappa}K_1(\kappa R) + \frac{C^*}{R}\right], \tag{B2}$$

$$C^* = \frac{1}{2(1-\phi)} - \frac{A_0}{2} - \frac{\kappa^2}{16} \tag{B3}$$

$$D = B(\log N - \log\phi - 1.4763), \tag{B4}$$

$$D^* = -\frac{\kappa^2}{4}\left(\frac{R^2}{4} - \frac{R^4}{16}\right) - \frac{A_0}{2}R^2(1 - \log R) + \frac{R^2}{4(1-\phi)} - C^*\log R + \frac{\beta K_0(\kappa R)}{k^*\kappa^2} + C\log R + D = B\log N + D_{ex}^*, \tag{B5}$$

$$D^*_{ex} = -\frac{\kappa^2}{4}\left(\frac{R^2}{4} - \frac{R^4}{16}\right) - \frac{A_0}{2}R^2(1-\log R) + \frac{R^2}{4(1-\phi)} - C^*\log R + \frac{\beta K_0(\kappa R)}{k^*\kappa^2} + C\log R - B(\log\phi + 1.4763), \tag{B6}$$

$$\langle\psi\rangle_{0,ex} = -\frac{B}{\kappa^2}(2\log R + \log\phi + 1.4763) + \left(\frac{1}{k^*\kappa^2} - \frac{1}{64}\right) \times \frac{\beta R K_1(\kappa R)}{2\kappa} + \frac{(\phi-3)A_0}{64} - \frac{\phi A_0(1-R^6)}{576} + \frac{B_0}{2}(R^2(1-\log R) - 1) + \frac{1-R^4}{64(1-\phi)} + \frac{A_0 R^4}{64}(3 - 2\log R - \phi) - \frac{K_0(\kappa R)}{\kappa K_1(\kappa R)} \times \left[\frac{2B}{\kappa^2 R} + \left(\frac{1}{k^*\kappa^2} - \frac{1}{64}\right)\frac{\beta R K_0(\kappa R)}{2} + \frac{\phi A_0 R^3}{16} - \frac{\phi A_0 R^5}{96} - \frac{B_0}{2}R(1-2\log R) - \frac{A_0}{32}R^3(5 - 4\log R) + \frac{R^3}{16(1-\phi)}\right] + \left(\frac{R^2-1}{4} + \frac{R}{2\kappa}\frac{K_0(\kappa R)}{K_1(\kappa R)}\right)D^*_{ex} \tag{B7}$$

References

[1] K.F. Jensen, Microreaction engineering – is small better? Chem. Engng. Sci. 56 (2001) 293–303.

[2] A.S. Sangani, A. Acrivos, Slow flow through a periodic array of spheres, Int. J. Multiphase Flow 8 (1982) 343–360.

[3] W. Wang, A.S. Sangani, Nusselt number for flow perpendicular to arrays of cylinders in the limit of small Reynolds and large Peclet numbers, Phys. Fluids 9 (1997) 1529–1539.

[4] E.M. Sparrow Jr., A.L. Loeffler, H.A. Hubbard, Heat transfer to longitudinal laminar flow between cylinders, J. Heat Transfer 83 (1988) 415–422.

[5] S. Koo, A.S. Sangani, Mass transfer coefficients for laminar longitudinal flow in hollow-fibre contactors, J. Fluid Mech. 484 (2003) 255–282.

[6] M.C. Yang, E.L. Cussler, Designing hollow-fiber contactors, AIChE J. 32 (1986) 1910–1916.

[7] D.L. Koch, J.F. Brady, Dispersion in fixed beds, J. Fluid Mech. 154 (1985) 399.

[8] A.S. Sangani, C. Yao, Transport processes in random arrays of cylinders. II. Viscous flow, Phys. Fluids 31 (1988) 2435–2444.

[9] H. Hasimoto, On the periodic fundamental solutions of the Stokes equations and their application to viscous flow past a cubic array of spheres, J. Fluid Mech. 5 (1959) 317–328.

[10] J. Happel, Viscous flow relative to arrays of cylinders, AIChE J. 5 (1959) 174–177.

[11] A.S. Sangani, C. Yao, Transport processes in random arrays of cylinders. I. Thermal conduction, Phys. Fluids 31 (1988) 2426–2434.

[12] T.L. Dodd, D.A. Hammer, A.S. Sangani, D.L. Koch, Numerical simulation of the effect of hydrodynamic interactions on diffusivities if integral membrane proteins, J. Fluid Mech. 293 (1995) 147–180.

[13] A.S. Sangani, G. Mo, Elastic interactions in particulate components with perfect as well as imperfect interfaces, J. Mech. Phys. Solids. 45 (1995) 2001–2031.

[14] P.D.M. Spelt, M. Norato, A.S. Sangani, M.S. Greenwood, L.L. Tavlarides, Attenuation of sound in concentrated suspensions: theory and experiments, J. Fluids Mech. 430 (2001) 51–86.

[15] D.G. Chae, F.H. Ree, T. Ree, Radial distribution functions and equation of state of the hard-disk fluid, J. Chem. Phys. 50 (1969) 1581–1589.

[16] A.S. Sangani, S. Behl, The planar singular solutions of Stokes and Laplace equations and their application to transport processes near porous surfaces, Phys. Fluids A1 (1989) 21–37.